

# Biobased Monoliths for Adenovirus Purification

Cláudia S. M. Fernandes,<sup>†,⊥</sup> Bianca Gonçalves,<sup>†,⊥</sup> Margarida Sousa,<sup>†,§,⊥</sup> Duarte L. Martins,<sup>‡</sup> Telma Barroso,<sup>†,§</sup> Ana Sofia Pina,<sup>†</sup> Cristina Peixoto,<sup>‡</sup> Ana Aguiar-Ricardo,<sup>\*,§</sup> and A. Cecília A. Roque<sup>\*,†</sup>

<sup>†</sup>UCIBIO, REQUIMTE, Departamento de Química, Faculdade de Ciências e Tecnologia, Universidade Nova de Lisboa, 2829-516 Caparica, Portugal

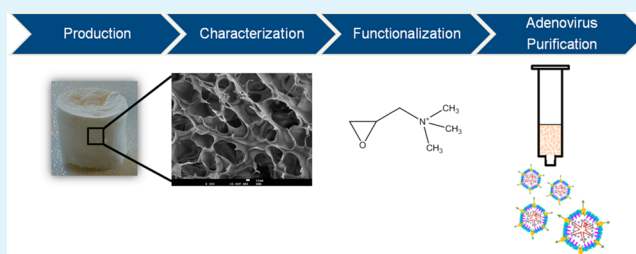
<sup>‡</sup>Instituto de Biologia Experimental Tecnológica, Avenida da República, Quinta do Marquês, Edifício IBET/ITQB, Estação Agronómica Nacional, 2780-157 Oeiras, Portugal

<sup>§</sup>LAQV, REQUIMTE, Departamento de Química, Faculdade de Ciências e Tecnologia, Universidade Nova de Lisboa, 2829-516 Caparica, Portugal

## Supporting Information

**ABSTRACT:** Adenoviruses are important platforms for vaccine development and vectors for gene therapy, increasing the demand for high titers of purified viral preparations. Monoliths are macroporous supports regarded as ideal for the purification of macromolecular complexes, including viral particles. Although common monoliths are based on synthetic polymers as methacrylates, we explored the potential of biopolymers processed by clean technologies to produce monoliths for adenovirus purification. Such an approach enables the development of disposable and biodegradable matrices for bioprocessing. A total of 20 monoliths were produced from different biopolymers (chitosan, agarose, and dextran), employing two distinct temperatures during the freezing process ( $-20\text{ }^{\circ}\text{C}$  and  $-80\text{ }^{\circ}\text{C}$ ). The morphological and physical properties of the structures were thoroughly characterized. The monoliths presenting higher robustness and permeability rates were further analyzed for the nonspecific binding of Adenovirus serotype 5 (Ad5) preparations. The matrices presenting lower nonspecific Ad5 binding were further functionalized with quaternary amine anion-exchange ligand glycidyltrimethylammonium chloride hydrochloride by two distinct methods, and their performance toward Ad5 purification was assessed. The monolith composed of chitosan and poly(vinyl) alcohol (50:50) prepared at  $-80\text{ }^{\circ}\text{C}$  allowed 100% recovery of Ad5 particles bound to the support. This is the first report of the successful purification of adenovirus using monoliths obtained from biopolymers processed by clean technologies.

**KEYWORDS:** monoliths, virus purification, cryogels, plasma processing, clean processes, biopolymers



## INTRODUCTION

The development of virus-based biopharmaceuticals for vaccination and gene therapy demands efficient purification methodologies.<sup>1</sup> Adenoviruses are intensively studied, as they are the preferred platform for gene therapy<sup>2</sup> and a very attractive choice for vaccinations.<sup>3,4</sup> Adenoviruses are  $2 \times 10^8$  Da nonenveloped particles containing linear double-stranded genomic DNA (26–45 kb) protected by a capsid. They exhibit icosahedral architecture with a diameter between 70 and 90 nm as determined by high-resolution techniques, including cryo-electron microscopy and X-ray crystallography.<sup>5,6</sup> Adenoviruses are an extremely appealing platform as they can be produced in high titers (1011 viral particles per milliliter), they do not integrate into the host cell genome, and they present potential for inserting DNA fragments up to 37 kb in length.<sup>2,5</sup> Several methods have been attempted for adenovirus purification, including CsCl density gradient ultracentrifugation, sucrose gradient ultracentrifugation, aqueous two-phase extraction, and ammonium sulfate precipitation. The purification of adenoviruses based on the CsCl method is very popular and simple as

it can yield fairly pure preparations.<sup>6</sup> Its major disadvantages relate to the toxicity of CsCl, which results in extensive dialysis of purified viral preparations, and to its limited applicability for large scale protocols. The CsCl method results in variable quality viral preparations, substantial loss of infectivity, and aggregation during storage.<sup>6</sup>

Adenovirus particles can be also separated through chromatography-based methodologies, where properties such as size, charge, hydrophobicity, and metal affinity are explored. Still, the most popular chromatographic protocol is based on the establishment of anion exchange interactions between the viral particles and the chromatographic matrix.<sup>1,6</sup> Currently available chromatographic matrices have pore dimensions that exclude viruses, suggesting that their adsorption is restricted to the bead surface area resulting in low binding capacities. This problem can be circumvented by tentacle supports, membrane

**Received:** December 17, 2014

**Accepted:** March 10, 2015

**Published:** March 10, 2015

chromatography, and, more recently, monolithic adsorbents. The latter are excellent for virus purification and removal due to the lower shear forces exerted on the viral particles. Monoliths consist of a solid continuous phase permeated by a network of pores, eliminating diffusion limitations. Convective transport is prevalent, which allows much faster volumetric throughput rates that in turn increases speed and productivity.<sup>8,9</sup> There are a wide range of processes and chemical functionalizations available for monolith preparations, which yield distinct microstructures, with variable pore sizes and geometries.<sup>10,11</sup> The high porosity and pore interconnections are common features of monoliths, which originate channels organized as a network.<sup>8</sup> Therefore, monoliths are very efficient for the purification of larger biomolecules and macromolecular complexes.<sup>4</sup> In fact, monoliths have been shown to be suitable for the purification of a wide range of viruses, including bacteriophages,<sup>12–14</sup> rubella viruses,<sup>15</sup> oncoretrovectors,<sup>17</sup> Adenovirus serotype 5,<sup>16</sup> and Adenovirus serotype 3.<sup>18</sup> Most of the monoliths used in the examples above are based on convective interaction media (CIM) technology by BIA Separations, GmbH. Other monolithic technologies are commercially available (e.g., UNO by Bio-Rad, Chromolith by Merck Millipore, Seprisorb by Sepragen, and SWIFT by ISCO); however, these represent expensive technologies and are mostly based on silica, acrylamide, or methacrylates.<sup>19,20</sup> We have recently shown that biopolymer-based monoliths are promising alternatives for biological purifications, namely for antibody molecules.<sup>19,21,22</sup> As these monoliths are prepared from biopolymers, they have certain advantages, including biodegradability, biocompatibility, and low-cost with significant potential for creating disposable components.

This work presents the production and characterization of monoliths that combine suitable morphological and physical characteristics with the potential for adenovirus binding and recovery. Monoliths were produced from different biopolymers, characterized, and tested for nonspecific binding of Adenovirus serotype 5 (Ad5). Matrices presenting lower nonspecific Ad5 binding were selected for further functionalization with quaternary amine anion-exchange ligand glycidyltrimethylammonium chloride hydrochloride (Q) by two methodologies, and lastly their performance toward Ad5 purification was assessed.

## EXPERIMENTAL SECTION

**1. Monolith Preparation by Freeze-Drying.** The monoliths were prepared by freeze-drying, and the exact composition of the casting solutions is detailed in Table 1. All described monoliths were prepared at least 10 times. Chitosan-based casting solutions were prepared as recently described.<sup>21,23</sup> In brief, acetic acid acidified water 1% (v/v, 3 mL) was employed for all chitosan-based casting solutions, and the remaining polymer casting solutions employed distilled water (3 mL). To each individual casting solution was added 11% (w/w polymer) of *N,N'*-methylenebis(acrylamide) (MBA, Fluka). The casting solutions were placed in individual 1.4 × 4.9 cm plastic tubes (with 1 mm wall thickness) and mixed with the aid of a magnetic stirrer. Distinct temperatures (20–90 °C), stirring velocities (300–800 rpm), and times (1–3 days) were employed, depending on the viscosity and water solubility of the biopolymers used. When homogenized, the initiator ammonium persulfate (APS, Merck, ≥98% purity; 42 μL of an aqueous solution at a concentration of 0.08 g/mL) and the catalyst *N,N,N',N'*-tetramethylethane-1,2-diamine (TEMED, Sigma-Aldrich; ≥99% purity; 23 μL) were added under stirring at 0 °C for either 30, or 30–45 min for chitosan- and dextran-based casting solutions, respectively, and at room temperature (25 °C) for 30 min for agarose-based solutions. Finally, all solutions were

**Table 1. Ratios of Monomer/Polymer Employed for Monolith Preparation<sup>a</sup>**

material	proportion (% w/w)	concentration (% w/w)	monolith denomination
chitosan	100	3.0	C3%
	100	2.0	C2%
chitosan/polyvinyl alcohol	50:50	3.0	C/P (50:50)
	33:67	3.0	C/P (33:67)
chitosan-glycidyl methacrylate	89:11	3.0	C-G
agarose-acrylamide-glycidyl methacrylate	56:7:37	4.5	A-AAm-G (56:7:37)
	58:12:30	5.4	A-AAm-G (58:12:30)
dextran-acrylamide-glycidyl methacrylate	56:7:37	4.5	D-AAm-G (56:7:37)
	49:14:37	4.5	D-AAm-G (49:14:37)
	58:12:30	5.4	D-AAm-G (58:12:30)
	52:17:30	5.4	D-AAm-G (52:17:30)

<sup>a</sup>Materials with a “/” denote a blend and a “-” denote copolymerization.

frozen at –20 °C and/or –80 °C for 24 h and then lyophilized (Telstar cryodos-50) for another 24 h or until they were dry (during the freeze-drying process, the lids of the vials were covered with paraffin film containing small holes).

**2. Monolith Characterization.** The determination of water fluxes was conducted under ambient conditions (22 °C and atmospheric pressure). The dried monolith samples were placed in a chromatography column with 0.64 cm<sup>2</sup> effective area and 6 cm height. Monoliths were wetted with distilled water (1 or 2 mL according to the swelling capacity). Then, 1 mL of distilled water was applied, and the time needed to flow through the column was recorded.<sup>21</sup> The water uptake capability of the materials was also tested as detailed in the Supporting Information (SI).

The porosity of the cryogels was estimated by a fluid displacement measurement method as previously reported,<sup>24,25</sup> which is further described in the SI. The porosity was calculated using eq 1.

$$\text{porosity (\%)} = \frac{\text{pore volume}}{\text{monolith volume}} \times 100 = \left[ \frac{w_1 - w_2}{\rho_{\text{ethanol}, 20^\circ\text{C}}} \right] \times 100 \quad (1)$$

The mechanical properties of all matrices were assessed at room temperature using tensile testing equipment (MINIMAT firmware v.3.1); monoliths were sliced into cylinders 0.75–1.20 cm in diameter and further subjected to uniaxial compression. Stress versus strain curves were built based on experimental data relating load to compression charts by applying eqs 2 and 3.<sup>21</sup> The compression modulus was then determined as the slope of the initial part of the stress–strain curve.<sup>21</sup>

$$\text{stress} = \sigma = \frac{F}{A} \quad (2)$$

$$\text{strain} = \varepsilon = \frac{\Delta l}{l} \quad (3)$$

where  $F$  corresponds to the applied force,  $A$  to the cross-sectional area,  $\Delta l$  to the change in length, and  $L$  to the clamps distance.

The morphology of the monoliths was assessed by scanning electron microscopy (SEM) using an accelerating voltage of 15 kV (Hitachi S 2400). Samples were frozen and fractured in liquid nitrogen for cross-sectional analysis. These were mounted on aluminum stubs using carbon discs (D-400, Neubaer Chemikalien) and gold-coated by sputtering prior to analysis. Then, micrographs were computationally segmented using ImageJ 20, allowing their posterior analysis to determine the average pore size diameter. All data was obtained from duplicated measurements (in the case of water flux measurements, each of the two samples were measured three times).

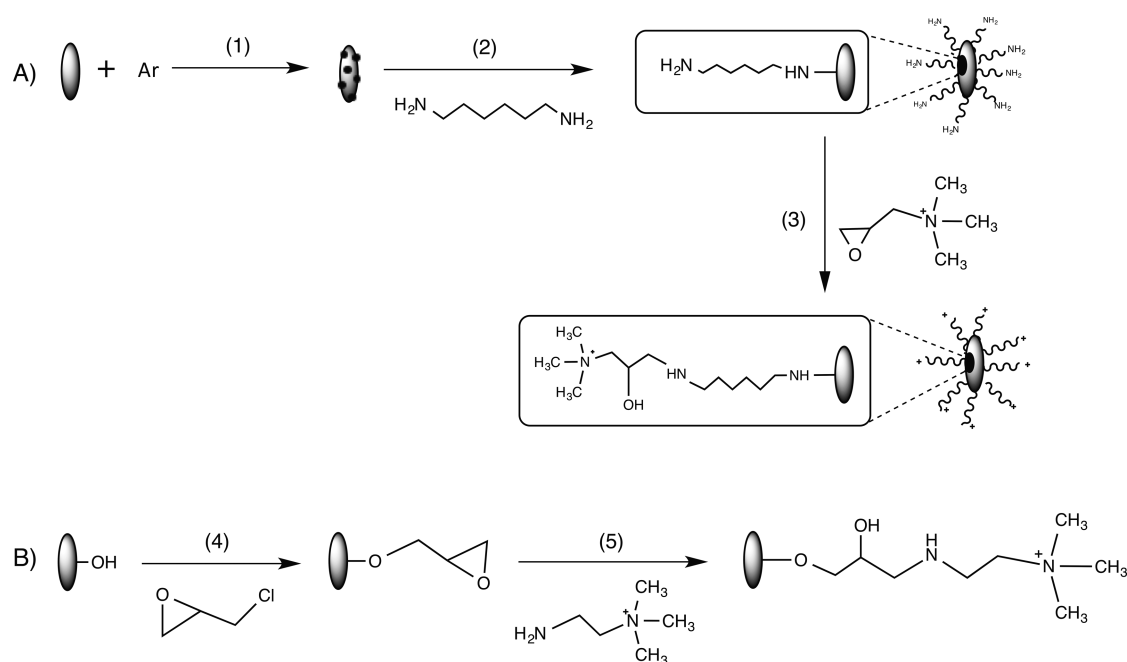


**Figure 1.** Schematic representation of monolith functionalization through the two methodologies. (A) In the plasma technique (M1), argon is applied to the monoliths to introduce radicals at the material surface (1), followed by amination with 1,6-hexanediamine (2) for subsequent Q ligand coupling (3). (B) In the epoxy-activation technique (M2), epoxy activation of the monoliths surface occurs upon the addition of epichlorohydrin (4) followed by coupling with the Q ligand (5).

**3. Monolith Amination by Plasma Technique and Ligand Q Coupling (Method 1).** Nonthermal plasma surface treatment of monoliths was employed to introduce amine groups within the monolith structure as described elsewhere<sup>21</sup> and summarized in Figure 1A. The monoliths were heated (150 °C) with agitation and placed in a radio frequency plasma reactor (FEMTO equipment, v. 3, Diener Electronics). A continuous flow of argon was then applied to reduce trace amounts of air and moisture. The monoliths were activated with argon (Ar)-plasma employing the following conditions: –60 W at a constant pressure of 0.3 Torr for 5 min, after which the plasma chamber was purged. For the amination stage, 1,6-hexanediamine contained in a flask at 150 °C was evaporated and inserted into the reaction chamber under vacuum for 30 min. The yield of amination was determined by the Kaiser Test.<sup>21</sup> For the first functionalization methodology (M1), Q ligand (5 mol excess in relation to the amine content) was dissolved in distilled water (10 mL) and 1 M NaOH (1 mol excess relative to the amine content) and added to the aminated monoliths, which then incubated for 16 h at 40 °C with agitation (200 rpm). After immobilization, the monoliths were thoroughly washed with distilled water.

**4. Monolith Epoxy Activation and Ligand Q Coupling (Method 2).** The second methodology (M2) was based on epoxy activation of the supports, as summarized in Figure 1B. Initially, a solution of 10 M NaOH (1 mL) was added to the monoliths (typically 40 mL/kg of moist cryogel) and incubated for 30 min at 30 °C with agitation (200 rpm). Then, epichlorohydrin (Sigma-Aldrich, 1 mL, typically 72  $\mu$ L/kg of moist cryogel) was added. The mixture was left incubating for 3 h at 36 °C (200 rpm). The monoliths were then washed five times with 10 mL of distilled water with agitation for 1 min. The extent of epoxy activation was determined as described previously.<sup>21</sup> For ligand immobilization, (2-aminoethyl)-trimethylammonium chloride hydrochloride ( $\text{NH}_2\text{-Q}$ , 5 mol excess relative to the epoxy activation yield) was dissolved in distilled water (5 mL) and 1 M NaOH (1 mol excess relative to the epoxy activation yield). The samples incubated overnight at 40 °C under stirring (200 rpm). After immobilization, the monoliths were thoroughly washed with distilled water.

**5. Ligand Q Quantification in the Monoliths.** Ligand quantification was assessed by a precipitation titration performed as

described in the literature<sup>26</sup> with a few modifications. The chloride ion capacity of the monoliths was determined by an argentometric titration with  $\text{AgNO}_3$  (0.1 M) combined with a silver ring electrode. This method is based on the reaction between  $\text{Ag}^+$  and  $\text{Cl}^-$  present in solution while the titrant is added. This results in the precipitation of  $\text{AgCl}$  particles. The amount of  $\text{AgNO}_3$  added corresponded to the number of moles of  $\text{Cl}^-$  released (100  $\mu$ mol/100  $\mu$ L added).

**6. Adenovirus Serotype 5 Production and Preclarification.** Ad5 viral bulk was produced in a stirred-tank bioreactor as described elsewhere.<sup>27</sup> The bioreactor was harvested and treated with 0.1% Triton X100 (Sigma-Aldrich, MO, USA) and incubated for 2 h at 37 °C with 50 U/mL of Benzonase (Merck-Millipore, Germany). Subsequently, the bulk was microfiltrated using 0.8  $\mu$ m + 0.45  $\mu$ m Sartopore 2 (Sartorius Stedim Biotech, Germany), concentrated 10-fold, and then subjected to five cycles of diafiltration with an R&D prototype Sartocoon cassette (Sartorius Stedim Biotech, Germany) with an average molecular weight cutoff of  $\sim$ 750 kDa. The bulk was stored in a buffer of 20 mM Tris-base and 150 mM NaCl pH 8 in aliquots at –80 °C until further use.

**7. Screening of Monolithic Structures toward Ad5 Virus Binding and Elution.** The monoliths were introduced in a Varian column (3 mL capacity) and incubated with distilled water (2 mL/cm of support) for 12 h to allow complete swelling of the material inside the chromatographic housing. The monoliths were further regenerated by washing five times with subsequent steps of regeneration buffer (2 mL, 0.1 M NaOH in 30% isopropanol) and distilled water (2 mL). Matrices were equilibrated in a buffer of 20 mM Tris-base and 150 mM NaCl pH 8 (5 mL; washing buffer). The Ad5 solution (1 mL, diluted 3-fold in washing buffer to a concentration of  $\sim$ 1.45  $\times$  10<sup>11</sup> total particles (TP)/mL) was then loaded onto the monoliths, followed by washing with the same buffer (20 mM Tris, 150 mM NaCl, pH 8). The Q-ligand functionalized monoliths were subsequently washed with elution buffer (20 mM Tris, 1 M NaCl, pH 8). Virus particle concentration, size distribution, and aggregation state were assessed by NanoSight NSS500 (NanoSight Ltd., U.K.; now Malvern Instruments, U.K.). Each sample was analyzed in triplicate, and the particles between 75 and 125 nm were considered. The percentage of adenoviruses unbound and eluted from the supports was calculated using eqs 4 and 5, respectively.



$$\text{unbound Ad5 (\%)} = \frac{\text{amount of washed Ad5 (TP)}}{\text{amount of loaded Ad5 (TP)}} \times 100 \quad (4)$$

$$\text{eluted Ad5 (\%)} = \frac{\text{amount of eluted Ad5 (TP)}}{\text{amount of loaded Ad5 (TP)}} \times 100 \quad (5)$$

## RESULTS AND DISCUSSION

**Morphological and Mechanical Characterization of Monoliths.** Fast flow rates and high recovery yields are desirable properties of robust porous supports employed for virus separations.<sup>28,29</sup> Ideal bioseparation supports must be hydrophilic, possess chemical and mechanical resistance, adequate porosity and interconnectivity. They must also present narrow pore size distribution and a high surface area with available functional groups.<sup>8,21,24</sup>

Three biological and biodegradable polymers, chitosan, dextran, and agarose, were used to produce monoliths. However, natural hydrophilic polymers tend to form soft structures with poor mechanical properties for chromatographic separations.<sup>30</sup> Therefore, a cross-linking agent (e.g., *N,N'*-methylenebis(acrylamide), MBA) was added to the casting solutions. Alternatively, synthetic polymers and monomers, such as poly(vinyl alcohol) (PVA), acrylamide, and/or glycidyl methacrylate (GMA), were blended with the biopolymers.

Before the lyophilization process, the homogenized casting solutions were cooled (0 °C) and polymerized thanks to the addition of the initiator ammonium persulfate (APS) and catalyst *N,N,N',N'*-tetramethylethane-1,2-diamine (TEMED) in a process called cryopolymerization.<sup>31,32</sup> Cryogels were obtained by freeze-drying as previously reported.<sup>21,33,34</sup> Water (vol %) is known to be a tuning parameter, and the casting solutions with concentrations in the range 2–6.7% (w/w) enhanced the highly interconnected open pore structure.<sup>35,36</sup> Previous works have reported the use of chitosan and agarose-based monoliths prepared at –80 °C for the efficient purification of antibody molecules.<sup>19,21</sup> In this work, because viral particles are considerably larger, the structures were also freeze-dried at –20 °C to increase the average pore size diameter of the monoliths produced.

Dynamic swelling assays were performed to assess the effect of copolymerization and blending of chitosan-based monoliths (detailed in Figures S1 and S2 in the SI). The amine groups of chitosan ( $\text{p}K_a \approx 6.3$ ) can change their protonation state as a function of pH changes in the surrounding environment.<sup>37</sup> Thus, chitosan-based monoliths presented changes in their swelling ability as a response to changes in the pH of the external environment. The remaining monoliths (dextran- and agarose-based) did not present structural variations upon pH changes, as these do not possess ionizable groups.<sup>38</sup>

The monoliths prepared presented porosities >89%, but no significant differences were observed for monoliths with the same compositions produced at –20 °C or at –80 °C (Table 2). Lowering the freezing temperature to –80 °C is expected to lower the water flux values due to a decrease in the average pore size.<sup>21</sup> The water flow is hindered by the reduced pore size (due to the higher surface area created), which increases the frictional force between fluid and material. The values of the compressive modulus in the hydrated state were lower than in the dry state, which is related to the higher mobility of network chains upon hydration. As the monoliths will be used in their hydrated states, these values correspond to a more realistic situation during the purification process. Comparing the same

**Table 2. Morphological and Mechanical Properties of the Prepared Monoliths**

monolith	porosity <sup>a</sup> (%)	water flux (L m <sup>-2</sup> h <sup>-1</sup> )	compressive modulus (kPa)	
			dry	hydrated
<i>T</i> <sub>freezing</sub> = –20 °C				
C3%	89 ± 3	79 ± 1	1.5 ± 0.4	0.3 ± 0.1
C2%	91 ± 2	<i>b</i>	2.6 ± 0.1	0.6 ± 0.1
C/P (50:50)	94.6 ± 0.3	150 ± 40	3.8 ± 0.1	0.7 ± 0.3
C/P (33.67)	93 ± 3	70 ± 20	4.3 ± 1.0	0.2 ± 0.04
C-G	93 ± 1	210 ± 20	3.7 ± 0.2	1.9 ± 0.1
A-Am-G (56:7:37)	95 ± 1	310 ± 60	1.76 ± 0.05	0.61 ± 0.04
A-Am-G (58:12:30)	95 ± 1	260 ± 40	5.0 ± 0.1	0.77 ± 0.05
D-AAm-G (56:7:37)	94.7 ± 0.5	150 ± 50	0.8 ± 0.1	0.25 ± 0.03
D-AAm-G (49:14:37)	<i>b</i>	<i>b</i>	<i>b</i>	<i>b</i>
D-AAm-G (58:12:30)	95 ± 2	90 ± 20	0.49 ± 0.05	0.3 ± 0.01
D-AAm-G (52:17:30)	<i>b</i>	<i>b</i>	<i>b</i>	<i>b</i>
<i>T</i> <sub>freezing</sub> = –80 °C				
C3%	91 ± 3	69 ± 8	4.1 ± 0.9	1.8 ± 0.3
C2%	90 ± 2	16 ± 0	1.9 ± 0.5	0.8 ± 0.1
C/P (50:50)	91.0 ± 0.4	70 ± 20	10 ± 1	1.7 ± 0.3
C/P (33.67)	90 ± 4	4 ± 1	10 ± 2	1.0 ± 0.3
C-G	91.0 ± 0.3	190 ± 40	7 ± 2	1.29 ± 0.05
A-Am-G (56:7:37)	<i>b</i>	<i>b</i>	<i>b</i>	<i>b</i>
A-Am-G (58:12:30)	<i>b</i>	<i>b</i>	<i>b</i>	<i>b</i>
D-AAm-G (56:7:37)	95.5 ± 0.3	3 ± 0	0.60 ± 0.04	<i>c</i>
D-AAm-G (49:14:37)	95 ± 3	13 ± 5	1.4 ± 0.5	<i>c</i>
D-AAm-G (58:12:30)	89 ± 4	50 ± 20	0.8 ± 0.1	1.0 ± 0.3
D-AAm-G (52:17:30)	96.4 ± 0.4	26 ± 1	1.0 ± 0.2	0.88

<sup>a</sup>Values obtained through Archimedes Principle. <sup>b</sup>Measurements were not possible due to low mechanical stability. <sup>c</sup>Values were impossible to measure due to thin thickness and wall rupture.

monoliths processed at different temperatures, those prepared at –80 °C presented higher compressive moduli, which are related to the formation of more compact and rigid materials. This was visible for most of the tested cryogel structures (Figure 2). The porosity and swelling capacity is usually higher for monoliths processed at higher temperatures (–20 °C) at the cost of lower stiffness.<sup>21</sup>

Comparing the monoliths blended with PVA and GMA, the latter yielded higher water permeability. Hydrophobic poly-GMA chains facilitated crystal growth through the reduction of casting viscosity, which contributes to larger pores, and through the exclusion of entangled copolymer from the frozen solvent due to its hydrophobicity. Therefore, larger ice crystals are formed, creating larger pores and consequently improved water flux. The monoliths presenting the best physical characteristics (high porosity, high water flux, and elevated compressive modulus values) were further characterized by SEM (Figure 3). These included C/P (50:50) and C-G prepared at –20 °C and –80 °C and agarose A-Am-G (58:12:30) prepared at –20 °C. C3% has also been analyzed for further comparison to assess

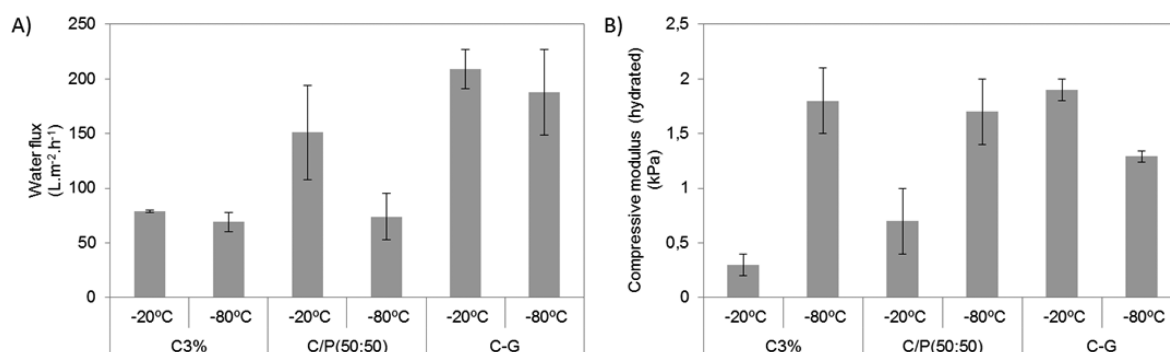


Figure 2. (a) Water flux ( $n = 3$ ) and (b) compressive modulus of the hydrated monoliths ( $n = 2$ ).

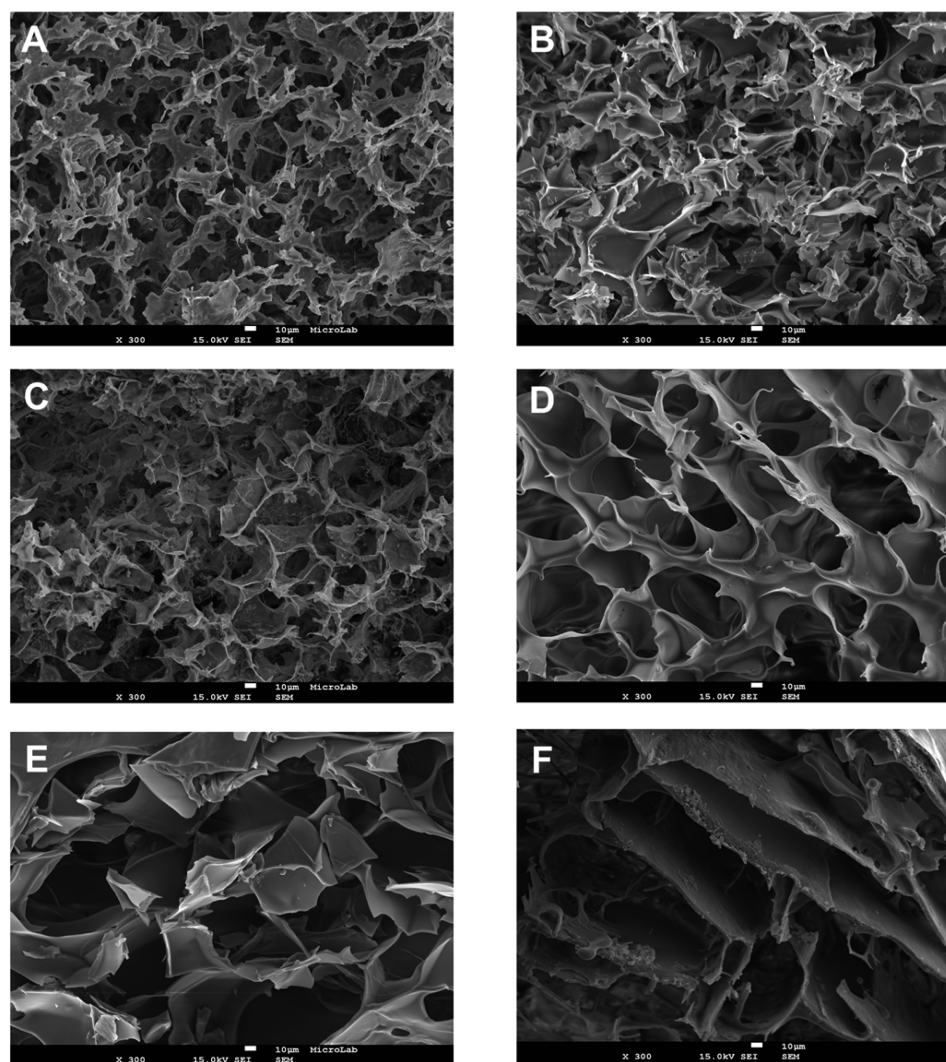


Figure 3. SEM micrographs (300 $\times$  magnification) of chitosan- and agarose-based monoliths prepared at  $-20$  °C (A, C and E) and  $-80$  °C (B, D, and F). (A) Ag-AAM-G (58:12:30), (B) C3%, (C and D) C/P (50:50), and (E and F) C-G.

how the polymerization with PVA and GMA altered the morphology and structure of the chitosan monolithic structure. Open pore microstructures with a high degree of interconnecting channels were visible in monoliths with a smooth surface produced by freezing and lyophilization processes. Freezing temperature tuned the average pore size, which is further reflected in the pore dimensions, as large pores are visible at  $-20$  °C and smaller pores are visible at  $-80$  °C, except for C/P (50:50). It was observed experimentally that the cryogels

produced at  $-20$  °C were fragile. Fracturing for SEM analysis was not efficient and led to structure destruction, which explains the differences in pore sizes. The C-G monoliths exhibited the smoothest surfaces, whereas the other supports presented with surface roughness, probably due to the dendritic morphology of the ice crystals. It was also possible to observe a difference in the pore architecture. In general, C-G monoliths derived from more viscous casting solutions yielded oval/semispherical pores. On the other hand, C/P (50:50) and Ag-

A-Am-G (58:12:30) presented more uniform pore structures (equiaxed). The high compression moduli of C-G can be attributed to its thick walls.

Comparing monoliths prepared by different polymers, it was clear that chitosan yields materials with higher stiffness and high water permeability. Agarose-based monoliths presented very high water permeability but were usually extremely fragile. As seen in the SEM images (Figure 3), agarose-based materials prepared at  $-20\text{ }^{\circ}\text{C}$  had a tracery appearance, which was also reflected in higher retention of viral particles (Figure 4). For

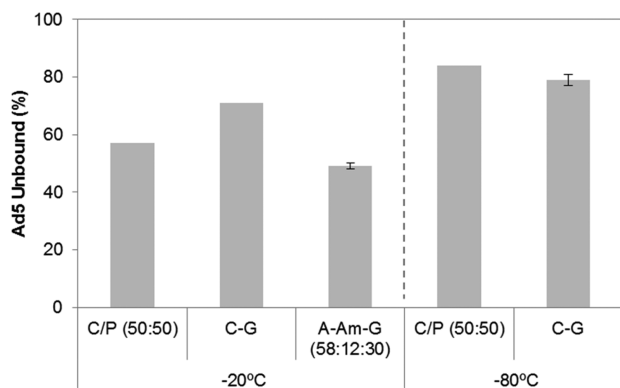


**Figure 4.** Comparison of adenovirus vector recovery using different nonfunctionalized monolithic supports. Unbound Ad5 percentages were calculated according to eq 4. Viral particle analysis was performed using a NanoSight NS500 instrument.

this reason, agarose monoliths prepared at  $-80\text{ }^{\circ}\text{C}$  were not tested for virus binding as they would yield smaller pores and even higher virus retention. The monoliths prepared from dextran were extremely fragile (as confirmed by the very low compressible modulus) with difficult handling and low water flux due to loss of integrity. Therefore, dextran-based monoliths were not considered for further tests with viral particles.

#### Selecting the Best Monoliths for Ad5 Purification.

Monoliths prepared with natural polymers give rise to hydrophilic surfaces, which are important during the chromatographic process to allow for the reversible adsorption of target biomolecules or particles and reduce unspecific binding. The high number of hydroxyl groups at the monolith's surface renders enough functional groups for further functionalization.<sup>10</sup> Agarose blended with acrylamide and glycidyl methacrylate (A-AAm-GMA (58:12:30)) frozen at  $-20\text{ }^{\circ}\text{C}$ , chitosan blended with glycidyl methacrylate (C-G), and chitosan blended with poly(vinyl alcohol) (C/P) frozen at  $-20\text{ }^{\circ}\text{C}$  and  $-80\text{ }^{\circ}\text{C}$  yielded the cryogels with the most promising physical and mechanical properties. However, it was still necessary to verify that these supports possess low nonspecific binding of Ad5 prior to support functionalization with the anion-exchange ligand. These data are summarized in Figure 4.

Upon comparing monoliths prepared at  $-20\text{ }^{\circ}\text{C}$  and  $-80\text{ }^{\circ}\text{C}$ , the former showed higher retention of Ad5, particularly for agarose-based monoliths, probably due to the fact that their internal pores presented tracery characteristics, as observed in the SEM images (Figure 3). However, SEM analysis can be dubious because the materials need to be fractured prior to analysis and the structures at  $-20\text{ }^{\circ}\text{C}$  were partially destroyed during this process. In fact, the low stiffness and robustness of the monoliths prepared at  $-20\text{ }^{\circ}\text{C}$  is most likely the critical

parameter that impedes their use in bioseparations, as the structures tend to collapse during the chromatographic run. Therefore, C/P (50:50) and C-G monoliths prepared at  $-80\text{ }^{\circ}\text{C}$  were chosen for further functionalization with an ion-exchange ligand typically employed in adenovirus purification and clearance.

**Monolithic Supports Applied for Ad5 Purification.** The viral particles of Ad5 are negatively charged as are most viruses. Anion-exchange chromatography employing quaternary amine ligands (Q ligands) is a typical purification protocol. In this work, two different functionalization methodologies were followed to introduce Q ligands at the monolith surface (see Figure 1). The plasma technique (M1) uses argon-plasma treatment to introduce radicals onto the support surface for subsequent amination with 1,6-hexanediamine and functionalization with the Q ligand. The amination yield obtained by plasma treatment was  $80 \pm 30\text{ }\mu\text{mol amines/g support}$  for C/P (50:50) monoliths and  $140 \pm 40\text{ }\mu\text{mol amines/g support}$  for C-G monoliths. The epoxy-activation method (M2) is based on the introduction of epoxy groups at the monolith surface. The epoxy-activation yield obtained was  $400 \pm 100\text{ }\mu\text{mol epoxy groups/g support}$  for C/P (50:50) monoliths and  $60 \pm 20\text{ }\mu\text{mol epoxy groups/g support}$  for C-G monoliths. The monoliths were modified with ligand Q following both M1 and M2 strategies and tested again for binding and elution of viral particles under the standard conditions employed in ion-exchange chromatography. The different monolithic materials were inserted into a chromatographic housing and loaded with 1 mL of Ad5 particles ( $\sim 1.45 \times 10^{11}\text{ TP/mL}$ ) followed by washing (20 mM Tris, 150 mM NaCl, pH 8) and elution (20 mM Tris, 1 M NaCl, pH 8). The results are shown in Figure 5.

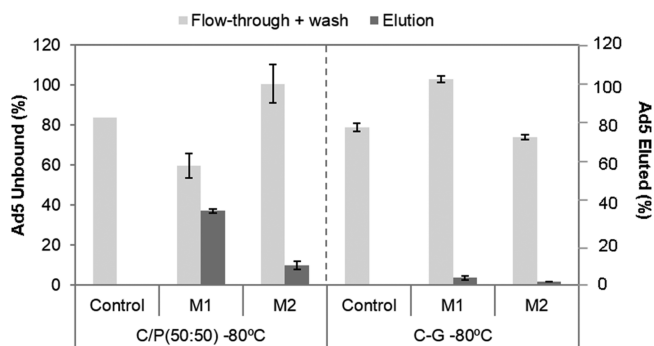


**Figure 5.** Comparative analysis of different functionalized and nonfunctionalized monolithic supports for adenovirus vector recovery concerning unbound and eluted Ad5. Control refers to nonfunctionalized supports (only washing results are displayed). M1 refers to functionalization of the previously aminated monoliths (plasma technique, Method 1). M2 refers to functionalization of the previously epoxy-activated monoliths (epoxy-activation technique, Method 2). The percentage of unbound Ad5 has been calculated according to eq 4, and the percentage of eluted Ad5 has been calculated according to eq 5. Viral particle analysis was performed using a NanoSight NS500 instrument.

C/P monoliths prepared at  $-80\text{ }^{\circ}\text{C}$  emerged as the most promising supports for Ad5 purification as it was possible to identify particles in the elution fraction. The amount of ligand Q immobilized in monoliths prepared by M1 and M2 was quantified for 20 and 200  $\mu\text{mol}$  of ligand Q/g support, respectively. It was found that monoliths prepared by M1 bound and eluted Ad5 particles more efficiently than monoliths



prepared by M2. This can be related to the two chemical routes followed, where M2 promotes covalent interactions between neighboring chains of polymers within the monolith structure, which entangle or immobilize ligand Q, making it inaccessible for interactions with the viral particles. The monolith C/P (50:50) prepared by M1 was able to retain ~40% of the loaded Ad5 particles after the washing procedure. Then, using elution conditions with a high salt concentration as is typically employed in anion-exchange chromatography of Ad5,<sup>39</sup> it was possible to desorb ~100% of the bound viral particles.

Contrastingly, functionalized C-G monoliths (M1) did not bind Ad5 particles and only 20% bound to the support prepared by M2. This result can be explained by the higher water flux observed for this cryogel structure, which did not promote interaction between the ligand and viral particles.

Ligand Q has also been reported to yield viral particle recovery between 33 and 70% when immobilized on commercial agarose matrices (e.g., HiTrap prepacked columns from GE Healthcare<sup>40</sup> and Mustang Chromatography Capsules from the Pall Corporation<sup>41</sup>). Other chromatographic methodologies have not achieved such good results. For example, monoliths functionalized with streptavidin allowed the recovery of only 8% of biotinylated oncovirus particles.<sup>17</sup> A maximum of 89% recovery of His-tag modified viral particles was achieved with membranes through immobilized metal affinity chromatography.<sup>42</sup> The best results reported in the literature were achieved with monolith CIM technology, which is based on immobilization of the Q ligand. It has demonstrated successful results for bacteriophage purification with yields of ~100,<sup>12</sup> 75, and 85%<sup>13</sup> or for the purification of rotavirus, rabies virus, lentivirus, measles, and mumps. CIM monoliths are prepared from glycidyl methacrylate-ethylenedimethacrylate or styrene-divinylbenzene, which are all non-natural polymers.<sup>13</sup> This work is the first report on the successful purification of adenoviruses using polymeric biodegradable cryogels, which are easily processed at low cost. It was also shown that biodegradable monoliths could be produced that allowed for the recovery of 100% of the bound viral particles.

## CONCLUSION

Several monolithic structures were obtained from biopolymers prepared at different freezing temperatures (−20 °C and −80 °C). The nonfunctionalized monoliths with the best physical and morphological characteristics were further tested against nonspecific binding to Ad5 viral particles. The monoliths presenting the lowest nonspecific binding were further modified and functionalized with ligand Q and tested for their applicability for Ad5 recovery by ion-exchange interactions. We describe for the first time the application of biopolymeric biodegradable monoliths for adenovirus purification. These monoliths can be easily produced in the laboratory with inexpensive reagents and clean technologies to yield nontoxic and biodegradable macroporous structures suitable for disposable bioseparation protocols. The C/P (50:50) monolith functionalized by plasma treatment yielded the best binding results and allowed for the elution of 100% of the bound viral particles. The eluted virus was in a colloidal solution meaning that the interaction with the monoliths and the exposure to washing and elution conditions did not lead to virus aggregation, which is an important quality attribute for virus-based products. Despite the encouraging results, further studies should envisage bioprocess engineering and development in terms of optimization of elution conditions for optimal virus activity

(dependent on each specific case) as well as maximization of the dynamic binding capacity. The monoliths produced can also be modified with different ligands for unique bioseparation purposes, thereby creating a toolbox that can be applied for the purification of several biologics, including other virus types, cells, organelles, large proteins, and nucleic acids.

## ASSOCIATED CONTENT

### Supporting Information

Experimental details for monolith characterization, in particular porosity determination, mechanical characterization, and swelling tests, as well as results and discussion of the swelling tests for different materials. This material is available free of charge via the Internet at <http://pubs.acs.org>.

## AUTHOR INFORMATION

### Corresponding Authors

\*E-mail: [air@fct.unl.pt](mailto:air@fct.unl.pt)

\*E-mail: [cecilia.roque@fct.unl.pt](mailto:cecilia.roque@fct.unl.pt)

### Author Contributions

<sup>†</sup>C.S.M.F., B.G., and M.S. contributed equally to this study.

### Funding

The authors are grateful to Fundação para a Ciência e Tecnologia (FCT), Portugal, for funding through Projects PEst-C/EQB/LA0006/2013, PTDC/EBB-BIO/118317/2010, and ERA-IB-2/0001/2013.

### Notes

The authors declare no competing financial interest.

## ACKNOWLEDGMENTS

The authors thank Prof. Rosário Bronze from Faculdade de Farmácia, Universidade de Lisboa.

## ABBREVIATIONS

SEM, scanning electron microscopy

Ad5, Adenovirus serotype 5

AAM, acrylamide

PVA, poly(vinyl alcohol)

GMA, glycidyl methacrylate

MBA, *N,N'*-methylenebis(acrylamide)

Q, glycidyltrimethylammonium chloride (a quaternary amine ligand)

Q-NH<sub>2</sub>, (2-aminoethyl)trimethylammonium chloride hydrochloride

M1, functionalization method based on previous amination of supports

M2, functionalization method based on previous epoxy activation of supports

## REFERENCES

- (1) Peixoto, C.; Ferreira, T. B.; Sousa, M. F.; Carrondo, M. J.; Alves, P. M. Towards Purification of Adenoviral Vectors Based on Membrane Technology. *Biotechnol. Prog.* **2008**, *24*, 1290–1296.
- (2) Ginn, S. L.; Alexander, I. E.; Edelstein, M. L.; Abedi, M. R.; Wixon, J. Gene Therapy Clinical Trials Worldwide to 2012—An Update. *J. Gene Med.* **2013**, *15*, 65–77.
- (3) Tatsis, N.; Ertl, H. C. Adenoviruses as Vaccine Vectors. *Mol. Ther.* **2004**, *10*, 616–629.
- (4) Podgornik, A.; Yamamoto, S.; Peterka, M.; Krajnc, N. L. Fast Separation of Large Biomolecules Using Short Monolithic Columns. *J. Chromatogr. B: Biomed. Sci. Appl.* **2013**, *927*, 80–89.
- (5) Volpers, C.; Kochanek, S. Adenoviral Vectors for Gene Transfer and Therapy. *J. Gene Med.* **2004**, *6* (Suppl 1), S164–S171.

- (6) Burova, E.; Ioffe, E. Chromatographic Purification of Recombinant Adenoviral and Adeno-Associated Viral Vectors: Methods and Implications. *Gene Ther.* **2005**, *12* (Suppl 1), S5–S17.
- (7) Jungbauer, A.; Hahn, R. Monoliths for Fast Bioseparation and Bioconversion and Their Applications in Biotechnology. *J. Sep. Sci.* **2004**, *27*, 767–778.
- (8) Gagnon, P. The Emerging Generation of Chromatography Tools for Virus Purification. *BioProcess Int.* **2008**, 1–5.
- (9) Fernandes, P.; Peixoto, C.; Santiago, V.; Kremer, E.; Coroadinha, A.; Alves, P. Bioprocess Development for Canine Adenovirus type 2 Vectors. *Gene Ther.* **2013**, *20*, 353–360.
- (10) Arrua, R. D.; Strumia, M. C.; Igarzabal, C. I. A. Macroporous Monolithic Polymers: Preparation and Applications. *Materials* **2009**, *2*, 2429–2466.
- (11) Svec, F. Porous Polymer Monoliths: Amazingly Wide Variety of Techniques Enabling their Preparation. *J. Chromatogr. A* **2010**, *1217*, 902–924.
- (12) Kramberger, P.; Honour, R. C.; Herman, R. E.; Smrekar, F.; Peterka, M. Purification of the *Staphylococcus aureus* Bacteriophages VDX-10 on Methacrylate Monoliths. *J. Virol. Methods* **2010**, *166*, 60–64.
- (13) Oksanen, H. M.; Domanska, A.; Bamford, D. H. Monolithic Ion Exchange Chromatographic Methods for Virus Purification. *Virology* **2012**, *434*, 271–277.
- (14) Adriaenssens, E. M.; Lehman, S. M.; Vandersteegen, K.; Vandenheuvel, D.; Philippe, D. L.; Cornelissen, A.; Clokie, M. R.; Garcia, A. J.; De Proft, M.; Maes, M.; Lavigne, R. CIM® Monolithic Anion-exchange Chromatography as a Useful Alternative to CsCl Gradient Purification of Bacteriophage Particles. *Virology* **2012**, *434*, 265–270.
- (15) Forcic, D.; Brgles, M.; Ivancic-Jelecki, J.; Santak, M.; Halassy, B.; Barut, M.; Jug, R.; Markušić, M.; Strancar, A. Concentration and Purification of Rubella Virus Using Monolithic Chromatographic Support. *J. Chromatogr. B: Biomed. Sci. Appl.* **2011**, *879*, 981–986.
- (16) Whitfield, R.; Battom, S.; Barut, M.; Gilham, D.; Ball, F. Rapid High-Performance Liquid Chromatographic Analysis of Adenovirus Type 5 Particles with a Prototype Anion-Exchange Analytical Monolith Column. *J. Chromatogr. A* **2009**, *1216*, 2705–2711.
- (17) Williams, S. L.; Eccleston, M. E.; Slater, N. K. Affinity Capture of a Biotinylated Retrovirus on Macroporous Monolithic Adsorbents: Towards a Rapid Single-Step Purification Process. *Biotechnol. Bioeng.* **2005**, *89*, 783–787.
- (18) Urbas, L.; Jarc, B. L.; Barut, M.; Zochowska, M.; Chroboczek, J.; Pihlar, B.; Szolajska, E. Purification of Recombinant Adenovirus type 3 Dodecahedral Virus-like Particles for Biomedical Applications using Short Monolithic Columns. *J. Chromatogr. A* **2011**, *1218*, 2451–2459.
- (19) Barroso, T.; Hussain, A.; Roque, A. C. A.; Aguiar-Ricardo, A. Functional Monolithic Platforms: Chromatographic Tools for Antibody Purification. *Biotechnol. J.* **2013**, *8*, 671–681.
- (20) Nordborg, A.; Hilder, E. F. Recent Advances in Polymer Monoliths for Ion-exchange Chromatography. *Anal. Bioanal. Chem.* **2009**, *394*, 71–84.
- (21) Barroso, T.; Roque, A. C. A.; Aguiar-Ricardo, A. Bioinspired and Sustainable Chitosan-based Monoliths for Antibody Capture and Release. *RSC Adv.* **2012**, *2*, 11285–11294.
- (22) Barroso, T.; Casimiro, T.; Ferraria, A. M.; Mattioli, F.; Aguiar-Ricardo, A.; Roque, A. C. A. Hybrid Monoliths for Magnetically-driven Protein Separations. *Adv. Funct. Mater.* **2014**, *24*, 4528–4541.
- (23) Barroso, T.; Temtem, M.; Hussain, A.; Aguiar-Ricardo, A.; Roque, A. C. A. Preparation and Characterization of a Cellulose Affinity Membrane for Human Immunoglobulin G (IgG) Purification. *J. Membr. Sci.* **2010**, *348*, 224–230.
- (24) O'Brien, F.; Harley, B. A.; Yannas, I. V.; Gibson, L. Influence of Freezing Rate on Pore Structure in Freeze-dried Collagen-GAG Scaffolds. *Biomaterials* **2004**, *25*, 1077–1086.
- (25) Ruiz, I.; Hermida, E. B.; Baldessari, A. Fabrication and Characterization of Porous PHBV Scaffolds for Tissue Engineering. *J. Phys.: Conf. Ser.* **2011**, *332*, 012028.
- (26) Gustavsson, P.-E.; Lemmens, R.; Nyhammar, T.; Busson, P.; Larsson, P.-O. Purification of Plasmid DNA with a New Type of Anion-exchange Beads Having a Non-Charged Surface. *J. Chromatogr. A* **2004**, *1038*, 131–140.
- (27) Nestola, P.; Silva, R. J.; Peixoto, C.; Alves, P. M.; Carrondo, M. J.; Mota, J. P. Adenovirus Purification by Two-column, Size-exclusion, Simulated Countercurrent Chromatography. *J. Chromatogr. A* **2014**, *1347*, 111–121.
- (28) Kirsebom, H.; Rata, G.; Topgaard, D.; Mattiasson, B.; Galaev, I. Y. Mechanism of Cryopolymerization: Diffusion-controlled Polymerization in a Nonfrozen Microphase. An NMR Study. *Macromolecules* **2009**, *42*, 5208–5214.
- (29) Wilson, P.; Heneghan, A.; Haymet, A. Ice Nucleation in Nature: Supercooling Point (SCP) Measurements and the Role of Heterogeneous Nucleation. *Cryobiology* **2003**, *46*, 88–98.
- (30) Jungbauer, A. Chromatographic Media for Bioseparation. *J. Chromatogr. A* **2005**, *1065*, 3–12.
- (31) Henderson, T. M.; Ladewig, K.; Haylock, D. N.; McLean, K. M.; O'Connor, A. J. Cryogels for Biomedical Applications. *J. Mater. Chem. B* **2013**, *1*, 2682–2695.
- (32) Jungbauer, A.; Hahn, R. Polymethacrylate Monoliths for Preparative and Industrial Separation of Biomolecular Assemblies. *J. Chromatogr. A* **2008**, *1184*, 62–79.
- (33) O'Brien, F.; Harley, B. A.; Yannas, I. V.; Gibson, L. Influence of Freezing Rate on Pore Structure in Freeze-dried Collagen-GAG Scaffolds. *Biomaterials* **2004**, *25*, 1077–1086.
- (34) Kumar, A.; Mishra, R.; Reinwald, Y.; Bhat, S. Cryogels: Freezing Unveiled by Thawing. *Mater. Today* **2010**, *13*, 42–44.
- (35) Jain, E.; Karande, A. A.; Kumar, A. Supermacroporous Polymer-based Cryogel Bioreactor for Monoclonal Antibody Production in Continuous Culture using Hybridoma Cells. *Biotechnol. Prog.* **2010**, *27*, 170–180.
- (36) Jain, E.; Kumar, A. Designing Supermacroporous Cryogels Based on Polyacrylonitrile and a Polyacrylamide-Chitosan Semi-Interpenetrating Network. *J. Biomater. Sci., Polym. Ed.* **2009**, *20*, 877–902.
- (37) Kathuria, N.; Tripathi, A.; Kar, K. K.; Kumar, A. Synthesis and Characterization of Elastic and Macroporous Chitosan-gelatin Cryogels for Tissue Engineering. *Acta Biomater.* **2009**, *5*, 406–418.
- (38) Jin, S.; Bian, F.; Liu, M.; Chen, S.; Liu, H. Swelling Mechanism of Porous P(VP-co-MAA)/PNIPAM Semi-IPN Hydrogels with Various Pore Sizes Prepared by a Freeze Treatment. *Polym. Int.* **2009**, *58*, 142–148.
- (39) Etzel, M. R.; Riordan, W. T. Viral Clearance Using Monoliths. *J. Chromatogr. A* **2009**, *1216*, 2621–2664.
- (40) Yamada, K.; McCarty, D. M.; Madden, V. J.; Walsh, C. E. Lentivirus Vector Purification Using Anion Exchange HPLC Leads to Improved Gene Transfer. *Biotechniques* **2003**, *34*, 1074–1078.
- (41) Slepishkin, V.; Chang, N.; Cohen, R.; Gan, Y.; Deausen, E.; Berlinger, D.; Binder, G.; Andre, K.; Humeau, L.; Dropulic, B. Large-scale Purification of a Lentiviral Vector by Size Exclusion Chromatography or Mustang Q Ion Exchange Capsule. *BioProcess. J.* **2003**, *2*, 89–95.
- (42) Opitz, L.; Hohlweg, J.; Reichl, U.; Wolff, M. W. Purification of Cell Culture-derived Influenza Virus A/Puerto Rico/8/34 by Membrane-based Immobilized Metal Affinity Chromatography. *J. Virol. Methods* **2009**, *161*, 312–316.